

Epoxy- and cyclopropane-functional copolymers: Synthesis, thermal properties and photocrosslinking behavior

VUSALA VAHABOVA*, KAZIM GULIYEV and ESFIRA ISKENDEROVA

Institute of Polymer Materials, Ministry of Science and Education of the Azerbaijan Republic, Sumgait, AZ5004, Azerbaijan

(Received 13 February, revised 23 March, accepted 21 April 2026)

Abstract: Copolymers bearing both epoxy and cyclopropane groups were synthesized by free-radical copolymerization of glycidyl 2-(4-vinylphenyl)cyclopropanecarboxylate (GVPCC) with methyl methacrylate (MMA) using AIBN at 343 K, in bulk and in benzene under inert atmosphere. Copolymer compositions were determined by spectroscopy and copolymerization parameters were evaluated by the Fineman–Ross method. The reactivity ratios were $r_1(\text{GVPCC}) = 0.68 \pm 0.05$ and $r_2(\text{MMA}) = 0.51 \pm 0.07$; their product ($r_1 r_2 = 0.35$) indicates random copolymerization with a tendency toward alternation. Alfrey–Price parameters ($Q_1 = 0.96$, $e_1 = -0.63$; $Q_2 = 0.74$, $e_2 = 0.40$) confirm strong comonomer interactions and pronounced polar effects. For a 50/50 copolymer, the intrinsic viscosity was 0.66 dL g^{-1} (benzene, $25 \text{ }^\circ\text{C}$). Thermogravimetric analysis showed composition-dependent stability with T_5 $250\text{--}320 \text{ }^\circ\text{C}$, increasing with GVPCC content, alongside improved adhesion (up to 5.6 MPa) and Vicat softening temperature ($121 \text{ }^\circ\text{C}$). UV irradiation produced efficient crosslinking and negative-tone photoresist behavior (resolution with depth of penetration, D_p $0.25\text{--}0.35 \text{ }\mu\text{m}$; critical exposure energy, E_c , $14.5\text{--}16.4 \text{ mJ cm}^{-2}$; sensitivity, S , $61\text{--}69 \text{ cm}^2 \text{ J}^{-1}$), demonstrating potential for UV-patternable microfabrication materials.

Keywords: cyclopropane ring; epoxy functionality; UV-induced crosslinking; negative-tone photoresist; working curve.

INTRODUCTION

As modern microelectronic technologies continue to advance, there is a growing demand for new functional polymeric materials with improved performance characteristics. Owing to their high thermal endurance, specific electrophysical properties and favorable deformation–strength behavior, such polymers are widely regarded as indispensable materials for forming protective and insulating layers in the fabrication of microelectronic devices.^{1–6}

* Corresponding author. E-mail: vusalavahabova@gmail.com
<https://doi.org/10.2298/JSC260213023V>

33 High-resolution topological patterns in polymer films are typically produced
34 by optical photolithography. In practice, two main strategies are used: either com-
35 plex multilayer resist systems are employed, or the intrinsic photosensitivity of the
36 polymer is exploited. Introducing built-in photosensitivity into the polymer matrix
37 is considered the more promising approach, since it can significantly simplify pro-
38 cessing and enhance the lithographic resolution. However, a persistent limitation
39 remains: most currently available resists exhibit insufficient photosensitivity,
40 which becomes a serious technological bottleneck.

41 To address this challenge and improve the lithographic performance of negat-
42 ive-tone photoresists, the synthesis of new monomers containing photoactive groups
43 – and the preparation of polymers based on these monomers – remains a highly
44 relevant task. In our earlier studies, the photochemical behavior of difunctional
45 substituted cyclopropylstyrenes was investigated.⁷ The present work represents a
46 logical continuation of those efforts and is focused on the radical copolymerization
47 of an epoxycarbonyl-substituted cyclopropylstyrene monomer, glycidyl 2-(4-vinyl-
48 phenyl) cyclopropanecarboxylate (GVPCC), with methyl methacrylate (MMA).

49 Although the photochemical properties of cyclopropyl-containing styrene
50 derivatives have been explored previously,^{8–12} the combined incorporation of an
51 epoxy functional group together with the cyclopropane fragment and, importantly,
52 its potential synergistic contribution to photosensitivity, has not been systematic-
53 ally examined. Here, we investigate this effect for the first time.

54 The main objective of this study is to elucidate the copolymerization behavior
55 of GVPCC and to systematically evaluate how the epoxycarbonyl substituent int-
56 roduced into the cyclopropane fragment of the side chain influences the photosen-
57 sitivity of the resulting macromolecules. The GVPCC monomer can be considered
58 a promising starting material for producing polymers with properties valuable for
59 microelectronic applications and, consequently, exhibits substantial potential for
60 further practical use.

61 EXPERIMENTAL

62 The target monomer, glycidyl 2-(4-vinylphenyl)cyclopropanecarboxylate (GVPCC), was
63 synthesized *via* the reaction of 2-(4-vinylphenyl)cyclopropanecarboxylic acid with epichloro-
64 hydrin (ECH) under basic conditions.

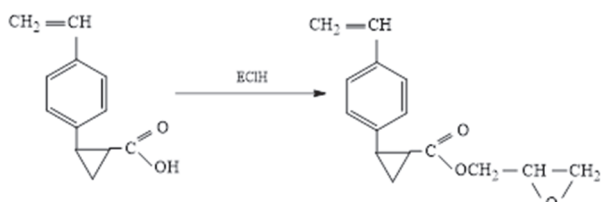
65 The synthesis was carried out by treating the acid with excess epichlorohydrin in the pre-
66 sence of sodium hydroxide, which facilitated the formation of the glycidyl ester through nucleo-
67 philic substitution and subsequent ring closure. The reaction proceeds *via* the intermediate chloro-
68 hydrin, followed by intramolecular cyclization to yield the epoxide-containing monomer.¹³

69 The overall synthetic route is presented in Scheme 1. The purity of the monomer was veri-
70 fied by gas chromatography (GC) and was found to be 99.8 %.

71 *Copolymerization procedure*

72 To evaluate the reactivity of the synthesized monomer and its potential for practical applic-
73 ations, it was subjected to radical copolymerization with methyl methacrylate (MMA). MMA,
74 99 % (Sigma–Aldrich) was used as received. The copolymerization of GVPCC with MMA was

75 carried out both in bulk and in benzene solution under a nitrogen atmosphere in sealed glass
76 ampoules.



77

78

Scheme 1. Synthesis of glycidyl 2-(4-vinylphenyl)cyclopropanecarboxylate (GVPCC).

79

80 After mixing the monomers with the initiator (azobisisobutyronitrile AIBN, 98 % Sigma-
81 Aldrich was used as received), the reaction mixture was transferred into a glass ampoule. The
82 mixture was purged with nitrogen for 8 min, after which the ampoule was tightly sealed and
83 maintained in a thermostat at 343 K. The initiator concentration was 0.3 wt. % relative to the
84 total monomer mass.

85

86

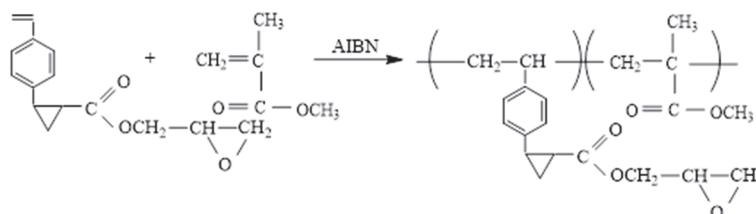
87

88

89

90

The resulting polymer was purified from benzene solution by double reprecipitation into
methanol and then dried under vacuum at 30 °C to constant mass at a residual pressure of 15-
20 mmHg. Benzene (99.5 %, Sigma-Aldrich) and methanol (99.8 %, Sigma-Aldrich) were
used as received. Yield: 259 mg (83 %, based on the total mass of monomers). The intrinsic
viscosity of the copolymers was measured in benzene at 25 °C using an Ubbelohde-type visco-
meter. The radical copolymerization of GVPCC with methyl methacrylate (MMA) initiated by
AIBN is shown in Scheme 2.



91

92

93

Scheme 2. AIBN-initiated radical copolymerization of GVPCC with methyl methacrylate
(MMA).

94

Characterization of the copolymers

95

96

97

98

99

100

101

102

103

104

105

106

¹H-NMR spectra were recorded on a Bruker AFR-300 spectrometer (300 MHz) in CDCl₃
using tetramethylsilane (TMS) as the internal standard; chemical shifts are reported in ppm (δ)
and coupling constants in Hz (J). FT-IR spectra were recorded on a Bruker Alpha FT-IR spec-
trometer (Germany). UV-Vis spectra were obtained on a Shimadzu UV-1800 spectrophoto-
meter in the 200–400 nm range. Thermogravimetric analysis (TGA) was performed under nitro-
gen on a NETZSCH TG 209 F3 Tarsus thermal analyzer at a heating rate of 10 °C min⁻¹.

Adhesion strength was determined by the pull-off method according to ISO 4624 using an
Elcometer 510 adhesion tester. Measurements were carried out on polymer films deposited on
glass plates at 23±2 °C with a loading rate of 1 MPa s⁻¹. The Vicat softening temperature was
determined according to ISO 306 (method B50) using a Vicat softening point apparatus at a
heating rate of 50 °C h⁻¹ under a load of 50 N. Tensile properties, including tensile strength and
elongation at break, were measured on a IM-4P (IM-4R) universal testing machine, AKIM-

107 -Metal, Russia, in accordance with ISO 527-2 at 23 °C and a crosshead speed of 10 mm min⁻¹.
 108 Impact resistance was evaluated by the Charpy method according to GOST 4647 using a MJI-09
 109 pendulum impact tester (Tochpribor, Russia) at room temperature.

110 *Method for evaluating the photosensitivity of the synthesized polymers*

111 Photoresist solutions containing the copolymers (4–13 wt. %) were prepared in benzene
 112 and spin-coated onto glass substrates at 2500 rpm. Film thickness after drying (room temp-
 113 erature followed by vacuum drying at 50 °C) was 0.20–0.25 μm (Linnik microinterferometer).
 114 UV exposure through a photomask was carried out using a DRT/DPT-220 mercury lamp (2.2
 115 A, 15 cm distance, 5–25 s), followed by development in dioxane:isopropyl alcohol (1:2 volume
 116 ratio) at 18–25 °C. Negative-tone behavior was confirmed by the insolubility of exposed areas
 117 in the developer. The surface exposure dose was calculated as:

$$118 \quad E_o = It \quad (1)$$

119 The critical exposure energy (E_c) and penetration depth (D_p) were obtained from the
 120 working curve:

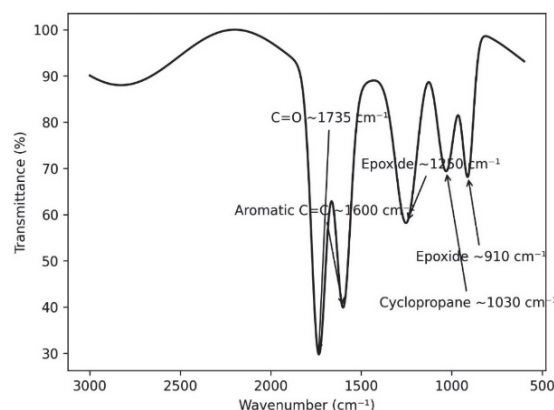
$$121 \quad C_d = D_p \ln(E_o / E_c) \quad (2)$$

122 where D_p is determined from the slope and E_c from the x -intercept.

123 RESULTS AND DISCUSSION

124 *Characterization of the copolymers*

125 The structure of the GVPCC–MMA copolymers synthesized in this work was
 126 supported by FTIR and ¹H-NMR spectroscopy. In the FTIR spectrum of the
 127 GVPCC monomer, the characteristic absorption bands of the vinyl group are
 128 clearly observed at 1630 and 990 cm⁻¹. After polymerization, the vinyl-group
 129 bands disappeared in the copolymer, indicating consumption of the double bond,
 130 while the intense bands assigned to the cyclopropane ring (1030–1035 cm⁻¹), the
 131 ester carbonyl group (1735 cm⁻¹) and the epoxide ring (910 and 1250 cm⁻¹)
 132 remain preserved. The FTIR spectrum of the GVPCC/MMA copolymer is shown in
 133 Fig. 1.



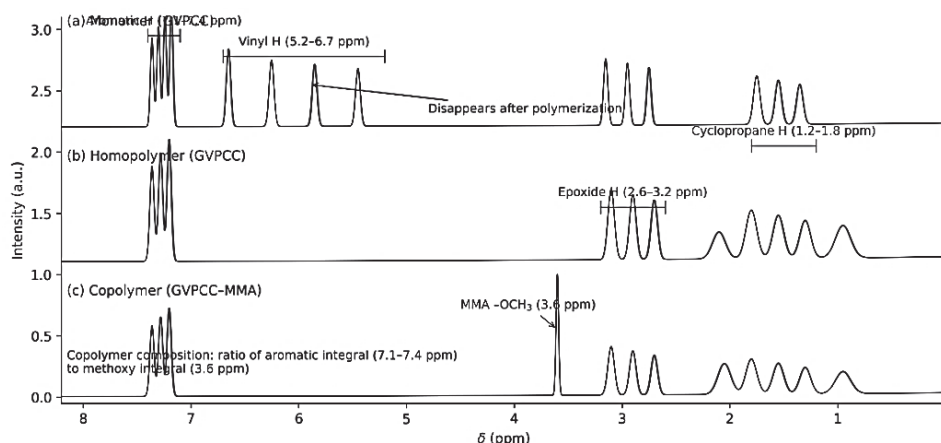
134
 135

Fig. 1. FTIR spectrum of the GVPCC/MMA copolymer.

136 A similar spectral pattern is observed for the copolymer. However, incorp-
 137 oration of MMA leads to an increase in both the intensity and the breadth of the
 138 ester carbonyl (C=O) absorption band in the 1725–1735 cm^{-1} region. This effect
 139 can be attributed to the overlap of carbonyl absorptions from two different ester
 140 functionalities present in the copolymer structure.

141 Comparative $^1\text{H-NMR}$ analysis

142 Comparative $^1\text{H-NMR}$ analysis was used to determine of the macromolecular
 143 composition. In the GVPCC monomer, the vinyl protons give distinct signals in
 144 the δ 5.2–6.7 ppm region. In the homopolymer, these signals were absent, demon-
 145 strating that polymerization proceeds *via* the vinyl double bond. The $^1\text{H-NMR}$
 146 spectrum of the GVPCC/MMA copolymer is shown in Fig. 2. The protons of the
 147 cyclopropane ring were observed at δ 1.2–1.8 ppm, while the epoxide-ring protons
 148 were detected in the δ 2.6–3.2 ppm range.



149

150 Fig. 2. Comparative $^1\text{H-NMR}$ spectra of the GVPCC monomer, its homopolymer and the
 151 GVPCC/MMA copolymer (CDCl_3 , 300 MHz).

152 In the copolymer spectrum, the signals characteristic of the GVPCC-derived
 153 units are retained and, in addition, a sharp singlet at δ = 3.6 ppm corresponding to
 154 the methoxy ($-\text{OCH}_3$) group of the MMA fragment appears. The mole ratio of the
 155 comonomer units in the copolymer was determined from the integral intensity ratio
 156 of the aromatic protons of GVPCC (δ 7.1–7.4 ppm) to the methoxy protons of MMA.

157 Copolymer composition and reactivity ratios

158 Copolymerization was carried out at various initial molar feed ratios of GVPCC
 159 and MMA. The composition of the resulting copolymers was determined by $^1\text{H-}$
 160 NMR spectroscopy based on the integral intensity ratio of the aromatic protons of
 161 the GVPCC units (δ 7.1–7.4 ppm) to the methoxy group of MMA (δ 3.6 ppm). It

162 was found that increasing the fraction of GVPCC in the initial feed led to a pro-
 163 portional increase in the content of epoxycarbonyl and cyclopropane fragments
 164 incorporated into the macromolecular chain.

165 To better understand the copolymerization behavior of the GVPCC/MMA
 166 system, the reactions were performed both in bulk and in benzene solution. Bulk
 167 polymerization made it possible to assess the behavior of the monomer pair in the
 168 absence of solvent, whereas solution polymerization in benzene provided lower
 169 viscosity and improved heat transfer, allowing better control of the reaction con-
 170 ditions. The obtained copolymerization results confirmed that GVPCC and MMA
 171 undergo efficient copolymerization, as reflected by the reactivity ratios $r_1 =$
 172 $= 0.68 \pm 0.05$ and $r_2 = 0.51 \pm 0.07$. Since both values are below unity and the product
 173 $r_1 r_2 = 0.35$, the system shows a tendency toward cross-propagation and partial
 174 alternation. Thus, the use of both bulk and solution conditions was helpful for
 175 evaluating the effect of the reaction medium on the copolymerization behavior and
 176 on the properties of the resulting copolymers.

177 As a quantitative characteristic of copolymerization, the relative reactivity of
 178 the monomers (reactivity ratios) was calculated using the Fineman–Ross method.¹⁴
 179 The compositions of GVPCC (M_1)/MMA (M_2) copolymers obtained at different
 180 initial feed ratios were determined by ¹H-NMR spectroscopy, and the results are
 181 summarized in Table I. The dependence of the copolymer composition on the
 182 initial monomer feed was well described by the Mayo–Lewis equation, showing
 183 good agreement with the experimental data.

184 TABLE I. Copolymer composition (mol %) for the GVPCC/MMA system

Sample No.	M_1 in feed	M_2 in feed	m_1 in copolymer	m_2 in copolymer
1	90	10	87.1	12.9
2	75	25	72.2	27.8
3	50	50	52.7	47.3
4	25	75	32.7	67.3
5	10	90	16.1	83.9

185 Fig. 3 illustrates the relationship between the initial monomer feed composition
 186 (M_1) and the resulting copolymer composition (m_1) for the GVPCC/MMA copoly-
 187 merization system. The deviation of the experimental points from the ideal $y = x$
 188 line indicates the occurrence of compositional drift during copolymerization and
 189 reflects differences in monomer reactivity during radical chain propagation. At low
 190 M_1 values, the fraction of monomer 1 in the copolymer is relatively higher ($m_1 >$
 191 $> M_1$), whereas at higher M_1 the data approach the ideal line ($m_1 \approx M_1$). These
 192 observations are consistent with reactivity ratios lower than unity ($r_1 < 1$ and $r_2 <$
 193 < 1) suggesting a preference for cross-propagation in the system and indicating a
 194 certain tendency toward alternating incorporation.

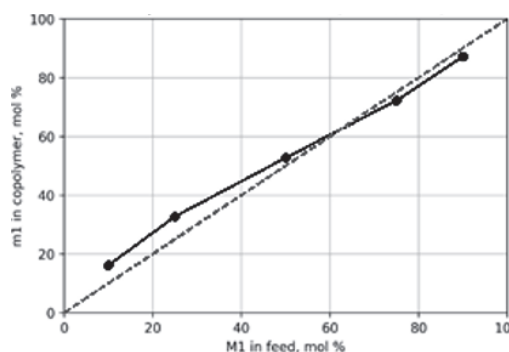


Fig. 3. Copolymer composition diagram for GVPCC/MMA: variation of m_1 as a function of the feed fraction M_1 .

195 Based on the Fineman–Ross analysis, the reactivity ratios were determined as
 196 $r_1 = 0.68 \pm 0.05$ for GVPCC and $r_2 = 0.51 \pm 0.07$ for MMA. Since both ratios are
 197 below unity ($r_1 < 1$ and $r_2 < 1$), each propagating radical preferentially adds the
 198 other monomer during chain growth. The fact that $r_1 > r_2$ indicates that the
 199 GVPCC-derived radical is more selective than the MMA-derived radical. Moreover,
 200 the product $r_1 r_2 = 0.35$, which is significantly lower than 1, suggests that the copoly-
 201 merization exhibits a tendency toward alternating incorporation on an otherwise
 202 statistical background.

203 To ensure reliable determination of the reactivity ratios (r_1 and r_2), copolymer-
 204 ization experiments were performed at low conversion (8–10 %), and the reactions
 205 were quenched at this stage to minimize composition drift.

206 Copolymer with a GVPCC:MMA feed mole ratio of 50:50 exhibited an intrinsic
 207 viscosity $[\eta]$ of $0.66 \text{ dL} \cdot \text{g}^{-1}$.

208 To assess the electronic and structural characteristics of the monomers, the
 209 Alfrey–Price scheme¹⁶ was applied to determine the Q and e parameters. For the
 210 GVPCC/MMA system, the reactivity ratios (r_1 and r_2) obtained at low conversion
 211 were used. The literature Q and e values for MMA were treated as fixed constants,
 212 and the Q and e parameters of GVPCC were back-calculated using the Alfrey–Price
 213 equations. For GVPCC, the values $Q = 0.96$ and $e = -0.63$ were obtained.

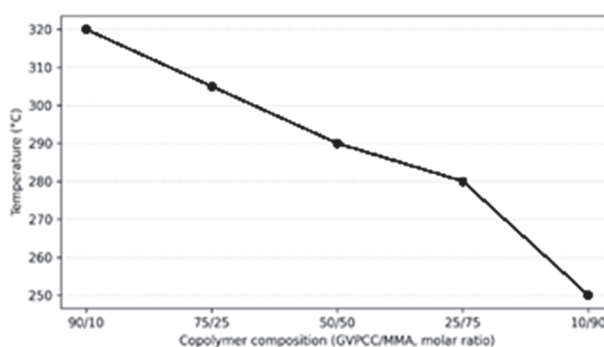
214 Compared with the commonly accepted literature values for MMA ($Q = 0.74$,
 215 $e = 0.40$) the higher Q value of GVPCC suggests enhanced resonance stabilization
 216 of the vinyl group, promoted by the aromatic ring and the cyclopropane fragment.
 217 The negative e parameter (-0.63) reflects the predominance of resonance effects
 218 that increase electron density in the monomer. Overall, these results indicate that
 219 GVPCC exhibits moderate reactivity and copolymerizes efficiently with MMA.
 220 The calculated parameters are summarized in Table II.

221 The thermal behavior of the synthesized GVPCC/MMA copolymers was
 222 investigated by thermogravimetric analysis (TGA). The TGA data indicate that
 223 thermal degradation proceeds through multiple steps. The initial weight-loss tem-
 224 perature (T_5 , corresponding to 5 % mass loss) was observed in the 250–320 °C

225 range depending on the copolymer composition: for GVPCC/MMA = 90/10,
 226 $T_5=320$ °C; for 75/25, $T_5 = 305$ °C; for 50/50, $T_5 = 290$ °C; for 25/75, $T_5 = 280$
 227 °C; for 10/90, $T_5 = 250$ °C (Fig. 4). These results demonstrate that increasing the
 228 GVPCC fraction enhances the thermal stability of the copolymers and confirms
 229 that the materials possess sufficiently high thermal resistance for microelectronic
 230 processing.

231 TABLE II. Monomer reactivity ratios and Alfrey–Price Q - e parameters for the GVPCC/MMA
 232 copolymerization system. Q_2 and e_2 values for MMA were taken from the literature; Q_1 and e_1
 233 for GVPCC were back-calculated using the Alfrey–Price scheme and the experimentally deter-
 234 mined reactivity ratios

System	Method	r_1 (GVPCC)	r_2 (MMA)	r_1r_2	Q_1	e_1	Q_2 (MMA)	e_2 (MMA)
GVPCC/MMA	Fineman–Ross	0.68 ± 0.05	0.51 ± 0.07	0.35	0.96	-0.63	0.74	0.40



235
 236
 237

Fig. 4. Thermogravimetric (TGA) profiles of GVPCC/MMA copolymers at various GVPCC:MMA ratios.

238 The observed improvement in stability can be attributed to strengthened intra-
 239 chain interactions promoted by the cyclopropane ring and aromatic moieties intro-
 240 duced into the side chains, which can hinder bond scission and slow down the
 241 overall decomposition process.

242 Table III shows that increasing the GVPCC comonomer content leads to a
 243 consistent improvement in both the thermal and mechanical performance of the
 244 MMA–GVPCC copolymers. When the GVPCC fraction is increased from 25 to
 245 75 mol %, the adhesion strength rises from 2.5 to 5.6 MPa (approximately a 2.24-
 246 -fold increase). This enhancement can be directly attributed to the structural fea-
 247 tures of the GVPCC units: the glycidyl epoxy ring and the ester linkage increase
 248 the overall polarity of the copolymer, thereby strengthening interfacial interactions
 249 with the substrate – particularly on surfaces bearing polar functional groups – through
 250 dipole–dipole interactions and hydrogen bonding. As a result, the interfacial bond-
 251 ing becomes more robust, leading to improved adhesion performance.

252 The Vicat softening temperature, used here as a measure of heat resistance, is
 253 also sensitive to the GVPCC content: 110 °C for 25 mol % GVPCC, 117 °C for 50
 254 mol % and 121 °C for 75 mol % (an overall increase of 11 °C). This trend can be
 255 attributed to the aromatic vinylphenyl fragment and the cyclopropane ring intro-
 256 duced by GVPCC, which restrict segmental chain mobility. As a result, the soft-
 257 ening temperature increases and the material exhibits improved dimensional stab-
 258 ility at elevated temperatures.

259 In terms of mechanical performance, the tensile strength increases from 68 to
 260 80 MPa (approximately +12 MPa, ~18 %). Importantly, this improvement is not
 261 achieved at the expense of brittleness; on the contrary, the elongation at break rises
 262 from 1.8 to 6.9 % (about a 3.8-fold increase). These results are consistent with a
 263 balanced structure–property effect in the copolymer: rigidifying fragments (aro-
 264 matic and cyclopropane units) enhance strength, while polar functionalities (ester
 265 and epoxy groups) promote local intermolecular interactions, enabling more effi-
 266 cient energy dissipation under deformation.

267 A similar trend is observed for impact resistance: with increasing GVPCC
 268 content, the value rises from 152 to 169 N·cm⁻¹ (an increase of 17 N·cm⁻¹, ~11 %).
 269 This improvement is consistent with the higher elongation at break and indicates
 270 enhanced resistance to damage under dynamic loading.

271 Overall, the results summarized in Table III demonstrate that increasing the
 272 GVPCC fraction leads to a comprehensive enhancement of the GVPCC/MMA
 273 copolymer properties: adhesion, heat resistance, strength, ductility, and impact res-
 274 istance all improve simultaneously. Although the highest performance is achieved
 275 for the sample containing 75 mol % GVPCC, a composition of 50 mol % GVPCC
 276 may represent a favorable compromise in terms of the heat-resistance–strength–
 277 –ductility balance, depending on the intended application.

278 TABLE III. Effect of GVPCC content (25–75 mol %) in MMA–GVPCC copolymers on
 279 adhesion strength, Vicat softening temperature (heat resistance), tensile strength, elongation at
 280 break and impact resistance

GVPCC content, M_1 / mol %	Adhesion strength, MPa	Vicat softening temp., °C	Tensile strength, MPa	Elongation at break, %	Impact resist- ance, N/cm
25	2.5±0.1	110±2	68±3	1.8±0.2	152±5
50	3.2±0.2	117±2	75±3	4.7±0.3	160±4
75	5.6±0.3	121±2	80±2	6.9±0.4	169±5

281 Values are given as mean ± standard deviation ($n = 3$). Overall, the data in
 282 Table III show a consistent improvement in adhesion, heat resistance, tensile strength,
 283 elongation at break and impact resistance with increasing GVPCC content.

284 Increasing the GVPCC fraction leads to a simultaneous rise in strength and
 285 elongation at break, suggesting that the “stiffness–ductility” balance in this system
 286 cannot be explained solely by chain rigidification. Rather, it is also associated with

287 enhanced intermolecular interactions that promote energy dissipation during defor-
288 mation. The aromatic ring and cyclopropane fragment within the GVPCC unit
289 restrict segmental rotational freedom and therefore act as rigid structural elements
290 that increase the load-bearing capacity (σ). At the same time, the ester (C=O) and
291 epoxy (C–O) functionalities increase the cohesive energy density of the copolymer
292 and can strengthen dipole–dipole attractions between chains, effectively creating
293 physical association points.

294 In addition, partial epoxy ring opening under processing conditions (*e.g.*, trace
295 moisture or catalytic impurities) is possible, which would generate –OH groups.
296 In such a case, reversible hydrogen bonds of the –OH \cdots O=C and –OH \cdots O– types
297 may form and act as additional “sacrificial” interactions. These dynamic bonds can
298 delay crack propagation and increase damping of mechanical energy during
299 stretching. The synergistic contribution of dipole–dipole interactions and hydrogen
300 bonding has been reported to improve both strength and toughness (energy absorp-
301 tion/elongation) in various polymer systems.¹⁷

302 Overall, the rigid fragments introduced by GVPCC (aromatic + cyclopropane)
303 enhance strength, while the polar functionality (ester/epoxy and potentially –OH
304 sites) reinforces dynamic interchain interactions, compensates for embrittlement,
305 and ultimately leads to the balanced mechanical response observed here.

306 The presence of multiple reactive functionalities of different chemical nature
307 within the synthesized copolymer chains (*e.g.*, epoxy, ether/ester, and cycloprop-
308 ane fragments) enhances both the photo-reactivity of the material and its potential
309 for further functional modification. These groups can facilitate the formation of cross-
310 links under UV irradiation and may also serve as “active sites” for subsequent
311 amination or other post-polymerization transformations. The synthesized GVPCC/
312 /MMA copolymers exhibited efficient UV-induced crosslinking and, according to
313 the insolubility criterion in the developer, showed negative-tone photoresist
314 behavior. A low critical exposure energy (E_c) indicates that network formation can
315 be initiated at a lower energy input, *i.e.*, the material displays high photosensitivity.
316 In this respect, the cyclopropane ring together with the epoxycarbonyl/ester func-
317 tionalities can be regarded as structural features that promote photochemical con-
318 version and accelerate network formation.

319 The copolymers also demonstrated high optical transparency ($T \approx 90\%$) which
320 is important for light propagation within the film and for maintaining process
321 stability during photopatterning. In addition, the refractive index $n_D^{20} = 1.583$ can
322 be attributed to the influence of the cyclopropane ring and ester/carbonyl-type
323 groups on polarizability and optical density in the macromolecular environment.
324 Taken together, these characteristics support the potential of the materials as thin-
325 film negative photoresists for applications in microelectronics and optoelectronics.

326 E_c decreased markedly with increasing copolymer concentration, from ~ 90
327 mJ cm^{-2} at 4 wt. % to $\sim 15 \text{ mJ cm}^{-2}$ at 13 wt. % (Fig. 5). This trend can be attributed

328 to the higher concentration of photoactive moieties (epoxy and cyclopropane frag-
329 ments) in the resist film at elevated polymer loadings, which reduces the minimum
330 energy required to initiate network formation under UV irradiation. Such a concen-
331 tration-dependent decrease in E_c confirms that the resist becomes more sensitive
332 at higher concentrations and can be viewed as a factor that improves energy effi-
333 ciency in microelectronic photoprocessing, as illustrated in Fig. 5.

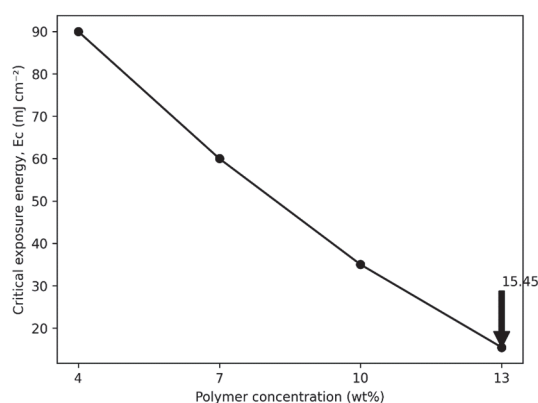


Fig. 5. Dependence of the critical exposure energy (E_c) on the concentration of the GVPCC/MMA copolymer.

334 The photoreactive behavior of the synthesized copolymer under UV irradi-
335 ation was investigated by UV-Vis spectroscopy (Fig. 6).

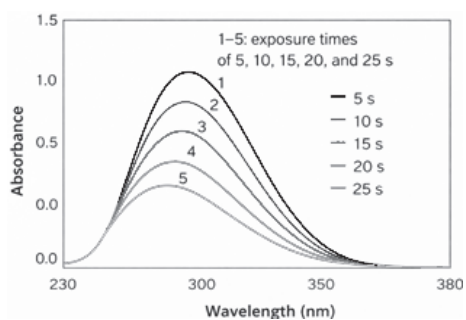


Fig. 6. UV-Vis spectra of the GVPCC/MMA copolymer recorded at different exposure times, showing the change in absorbance intensity.

336 UV-Vis spectra showed a progressive decrease of the absorption band at 296-
337 -300 nm as the exposure time increased from 5 to 25 s, indicating consumption of
338 photoactive fragments and advancement of crosslinking. Similar trends have been
339 reported as a sensitive marker of photopolymerization progress.¹⁸ The combined
340 presence of epoxy and cyclopropane units enhances the photochemical response,
341 which is reflected in the working-curve parameters (E_c and D_p). Under the emp-
342 loyed conditions (15 cm distance), 5-25 s exposure was sufficient to obtain stable
343 negative-tone patterns in 0.20-0.25 μm films, as confirmed by optical microscopy.

344 The measured D_p values (0.25–0.35 μm) are comparable to the film thickness,
 345 suggesting that light may penetrate the entire film and cause dose redistribution
 346 due to substrate reflection; therefore, thicker films (0.5–1.0 μm) or the use of UV-
 347 -absorbing additives could improve process robustness. FTIR spectra also support
 348 photostructuring, showing a decrease in bands attributed to the epoxide/cyclo-
 349 propane-related vibrations and the carbonyl group upon irradiation, consistent with
 350 network formation. The crosslinking is likely promoted by UV activation of epoxy
 351 groups and possible cyclopropane-involving radical processes, resulting in an
 352 insoluble 3D network responsible for negative development behavior.

353 Because the epoxide ring is a highly reactive functional group, it may partic-
 354 ipate in ring-opening reactions initiated by photo-generated active centers, depending
 355 on the formulation and surrounding medium. This interpretation is consistent with
 356 the decreased intensity of epoxide-related FTIR bands and supports the assumption
 357 that epoxide groups contribute to the crosslinking process. An increased network
 358 (gel) density may, in turn, enhance film rigidity and help explain why structuring
 359 occurs at relatively low exposure doses (low E_c) in the working-curve analysis
 360 (Fig. 7).

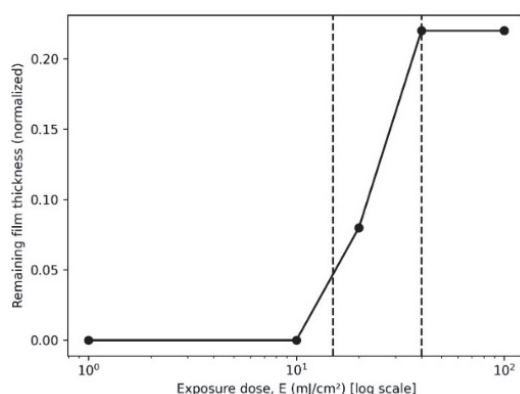


Fig. 7. Working curve of the GVPCC/MMA negative-tone photoresist: remaining film thickness after development (d) as a function of exposure dose (E , mJ/cm^2). The critical dose is $E_c = 15.5 \text{ mJ}/\text{cm}^2$, and the effective optical penetration depth, D_p , is 0.25–0.35 μm (film thickness: 0.20–0.25 μm).

361 At the same time, epoxide groups can remain available as reactive sites for
 362 amination and other post-polymerization transformations, enabling further post-
 363 -functionalization of the material.

364

CONCLUSION

365 In this work, free-radical copolymerization of the epoxy- and cyclopropane-
 366 -functional monomer GVPCC with methyl methacrylate (MMA) was carried out,
 367 and the composition/structure of the resulting copolymers was confirmed by FTIR
 368 and $^1\text{H-NMR}$ spectroscopy. Reactivity ratios determined by the Fineman–Ross
 369 method were $r_1(\text{GVPCC}) = 0.68 \pm 0.05$ and $r_2(\text{MMA}) = 0.51 \pm 0.07$ ($r_1 r_2 = 0.35$),

370 indicating that the system exhibits a tendency toward alternating incorporation on a
371 predominantly statistical copolymerization background.

372 Thermogravimetric analysis showed that the thermal stability of the copoly-
373 mers depends on composition: the temperature corresponding to 5 % mass loss
374 (T_5) ranged from 250 to 320 °C and increased with increasing GVPCC content
375 (e.g., 10/90 → 250 °C, 50/50 → 290 °C, 90/10 → 320 °C). Increasing the GVPCC
376 fraction from 25 to 75 mol % resulted in an overall improvement in both thermal
377 and mechanical performance: adhesion strength increased from 2.5 to 5.6 MPa and
378 the Vicat softening temperature rose from 110 to 121 °C. At the same time, tensile
379 strength increased from 68 to 80 MPa without a loss in ductility; instead, elongation
380 at break increased from 1.8 to 6.9 %, accompanied by an increase in impact resist-
381 ance from 152 to 169 N·cm⁻¹.

382 The copolymers exhibited efficient UV-induced crosslinking and negative-tone
383 photoresist behavior. Working-curve analysis gave D_p 0.25–0.35 μm and E_c 14.5–
384 –16.4 mJ·cm⁻² (S 61–69 cm²·J⁻¹), confirming the high photosensitivity of the
385 materials. Overall, combining epoxy and cyclopropane functionality provides a pro-
386 mising functional polymer platform for microelectronic applications, offering imp-
387 roved mechanical/thermal properties together with UV patternability.

388 *Acknowledgements.* The experimental work (polymer synthesis and characterization) was
389 carried out at the Institute of Polymer Materials, Ministry of Science and Education of the
390 Republic of Azerbaijan (Sumgayit, Azerbaijan). The authors gratefully acknowledge the Instit-
391 ute for access to instrumentation and laboratory facilities.

ИЗВОД

ЕПОКСИ- И ЦИКЛОПРОПАН-ФУНКЦИОНАЛНИ КОПОЛИМЕРИ: СИНТЕЗА, ТОПЛОТНА СВОЈСТВА И ПОНАШАЊЕ ПРИ ФОТОУМРЕЖАВАЊУ

VUSALA VAHABOVA*, KAZIM GULIYEV и ESFIRA ISKENDEROVA

*Institute of Polymer Materials, Ministry of Science and Education of the Azerbaijan Republic, Sumgayit,
AZ5004, Azerbaijan*

398 Кополимери са епоксидним и циклопропанским групама синтетизовани су кополи-
399 меризацијом глицидил-2-(4-винилфенил)циклопропанкарбоксилата полимеризацијом
400 слободним радикалима (GVPCC) са метил-метакрилатом (ММА) користећи АІВN на 343
401 К, у маси и бензену под инертном атмосфером. Састави кополимера су одређени спек-
402 троскопијом, а параметри кополимеризације су процењени Fineman–Ross методом.
403 Коефицијенти реактивности су били $r_1(\text{GVPCC}) = 0,68 \pm 0,05$ and $r_2(\text{ММА}) = 0,51 \pm 0,07$;
404 њихов производ ($r_1 r_2 = 0,35$) указује на статистичку кополимеризацију са тенденцијом ка
405 наизменичној. Alfrey–Price параметри ($Q_1 = 0,96$, $e_1 = -0,63$; $Q_2 = 0,74$, $e_2 = 0,40$) потврђују
406 јаке интеракције комономера и изражене поларне ефекте. За 50/50 кополимер, интри-
407 зична вискозност је 0,66 dL g⁻¹ (бензен, 25 °C). Термогравиметријска анализа показала је
408 стабилност зависну од састава са T_5 250–320 °C, која се повећава са GVPCC садржајем, уз
409 побољшану адхезију (до 5,6 МПа) и Викатову температуру омекшавања (121 °C). UV
410 зрачење је произвело ефикасно умрежавање и понашање фоторезиста негативног тона
411 (резолюција са дубином пенетрације, D_p , 0.25–0.35 μm; критична енергија излагања, E_c ,

412 14,5–16,4 mJ cm⁻²; осетљивост, S, 61–69 cm² J⁻¹), демонстрирајући потенцијал за микро-
413 фабрикацију материјала за UV узорке.

414 (Примљено 13. фебруара, ревидирано 23. марта, прихваћено 21. априла 2026)

415

REFERENCES

- 416 1. Q. Lin, *Polymer* **286** (2023) 126395 (<https://doi.org/10.1016/j.polymer.2023.126395>)
417 2. C. Ober, K. Käfer, F. Yuan, Ch., *Polymer* **280** (2023) 126020
418 (<https://doi.org/10.1016/j.polymer.2023.126020>)
419 3. R. Zhou, M. Cao, Y. Tan, M. Neisser, H. Xu, *Sci. Adv.* **11**(29) (2025) 1918
420 (<https://doi.org/10.1126/sciadv.adx1918>)
421 4. Y. Wang, H. Yu, L. Wang, Y. Zhang, Z. Zhu, Y. Zhang, Y. Lu, Ch. Ouyang, *J. Mat.*
422 *Chem., A* **13** (2025) 29860 (<https://doi.org/10.1039/D5TA04194E>)
423 5. Y. J. Wan, G. Li, Y. M. Yao, X. L. Zeng, P. L. Zhu, R. Sun, *Comp. Comm.* **19** (2020) 154
424 (<https://doi.org/10.1016/j.coco.2020.03.011>)
425 6. Y. Wen, C. Chen, Y. Ye, Z. Xue, H. Liu, X. Zhou, Y. Zhang, D. Li, X. Xie, Y. Mai, *Adv.*
426 *Mat.* **34** (2022) e2201023 (<https://doi.org/10.1002/adma.202201023>)
427 7. K. G. Guliyev, G. Z. Ponomareva, Kh. G. Nazaraliyev, A. M. Guliyev, *Azerb. Khim. Zh.*
428 **1** (1999) 87 (in Russian)
429 8. K. G. Guliev, G. Z. Ponomareva, Kh. G. Nazaraliev, A. M. Guliev, *Azerb. Khim. Zh.* **1**
430 (1999) 87 (in Russian)
431 9. K.G. Guliyev, S.B. Mamedli, T.S.D. Gulverdashvili, A.M. Guliyev, *Applied Chemistry*
432 *and Chemical Engineering*, Vol. 2, Apple Academic Press, Palm Bay, FL, 2017
433 10. A. I. Sadygova, *Azerbaijan Chem. J.* **3** (2022) 45 (<https://akj.az/en/journals/949>)
434 11. M. Sayes, G. Benoit, A. B. Charette, *Angew. Chem. Int. Ed.* **57** (2018) 13514
435 (<https://doi.org/10.1002/anie.201807347>)
436 12. K. Mizuno, N. Ichinose, Y. Yoshimi, *J. Photochem. Photobiol., C* **1** (2000) 167
437 ([https://doi.org/10.1016/S1389-5567\(00\)00011-3](https://doi.org/10.1016/S1389-5567(00)00011-3))
438 13. K.G. Guliev, G.Z. Ponomareva, A. M. Guliev, *Vysokomolekulyarnye soedineniya, B* **49**
439 (2007) 1577 (in Russian)
440 14. M. Fineman, S. D. Ross, *J. Polymer Sci.* **5** (1950) 259
441 (<https://doi.org/10.1002/pol.1950.120050210>)
442 15. F. R. Mayo, F. M. Lewis, *J. Am. Chem. Soc.* **66** (1944) 1594
443 (<https://doi.org/10.1021/ja01237a052>)
444 16. T. Alfrey Jr., C. C. Price, *J. Polymer Sci.* **2** (1947) 101
445 (<https://doi.org/10.1002/pol.1947.120020112>)
446 17. Y. Zhang, Y. Li, W. Liu, *Adv. Funct. Mat.* **25** (2015) 471
447 (<https://doi.org/10.1002/adfm.201401989>)
448 18. J. Bennett, *Addit. Manuf.* **18** (2017) 203 (<https://doi.org/10.1016/j.addma.2017.10.009>).